IOP Publishing Journal of Physics: Condensed Matter
J. Phys.: Condens. Matter **26** (2014) 135901 (9pp) doi:10.1088/0953-8984/26/13/135901

Marble game with optimal ferroelectric switching

J Cole[1,2], S J Ahmed[1,2], L Curiel[1,2], S Pichardo[2,3] and O Rubel[1,2]

[1] Thunder Bay Regional Research Institute, 980 Oliver Road, Thunder Bay, Ontario P7B 6V4, Canada
[2] Lakehead University, 955 Oliver Road, Thunder Bay, Ontario P7B 5E1, Canada
[3] Sunnybrook Health Sciences Centre, 2075 Bayview Ave., Toronto, Ontario M4N 3M5, Canada

E-mail: rubelo@tbh.net

Received 2 December 2013, revised 30 January 2014
Accepted for publication 14 February 2014
Published 13 March 2014

Abstract

A low coercivity and, consequently, low hysteresis loss are desired properties for ferroelectric materials used in high-power and high-frequency actuators. The coercive field required for the onset of ferroelectric switching is shown to develop a strong directional anisotropy due to peculiarities of an energy surface associated with the polarization rotation. It is found that the ferroelectric anisotropy exhibits 'hard' and 'easy' switching axes similar to magnetic materials. The hard axis corresponds to 180° polarization reversal, whereas the easy axis favors 90° switching. Our results suggest that the intrinsic low coercivity and the full polarization reversal may not be achieved at the same time under uniaxial excitation. A rotating electric field excitation is proposed in order to circumvent this limitation and to guide the polarization switching along a curved path.

Keywords: ferroelectric switching, polarization, coercive field, anisotropy, density-functional theory

(Some figures may appear in colour only in the online journal)

1 Introduction

Lead-based perovskites $PbZr_xTi_{1-x}O_3$ (PZT) have emerged as one of the most widely studied and technologically important class of ferroelectric oxides. This alloy exhibits an enhancement of electromechanical response near to the morphotropic phase boundary (MPB) at $x \approx 0.4$–0.5 that exceeds by far the properties of individual constituents $PbZrO_3$ and $PbTiO_3$. The enhancement of the piezoelectric response near MPB is attributed to 'flattening' of an energy surface that facilitates inversion of the spontaneous polarization [1–4].

A simplified scenario of the polarization inversion involves a structural transformation with an intermediate transition via the centrosymmetric (cubic) structure with zero polarization [5–7]. This process, also referred to as an Ising-type switching, corresponds to a 180° flip of polarization and requires overcoming of a large energy barrier, since the centrosymmetric structure is unfavorable below the Curie temperature.

A polarization rotation mechanism was proposed by Fu and Cohen [8] as an alternative to the polarization flip. During the structural transformation associated with the polarization rotation, the polarization vector $\boldsymbol{P}$ does not vanish, but rather changes its direction while maintaining the magnitude almost identical to the spontaneous polarization. The energy barrier for polarization rotation can be 2–3 times lower than the barrier associated with the flip of polarization [8–11]. Although, the barrier height argument seems to be physically relevant, the figure of merit for ferroelectric switching is the coercive field (the thresholds at which the switching occurs).

In this communication we investigate the single-domain ferroelectric switching in $PbTiO_3$ by polarization rotation. We observe a strong anisotropy of the coercive field, which originates from a peculiar free-energy surface for polarization inversion. Furthermore, it is possible to reduce coercivity and, consequently, the energy dissipation during the operation of ferroelectric transducers by introducing a rotating electric field instead of the traditional uniaxial excitation.

The paper is structured as follows. First, we identify structural transformations for the polarization inversion in $PbTiO_3$ and map the associated energy surface (section 2). Obtained results are used to justify Landau–Devonshire (LD)

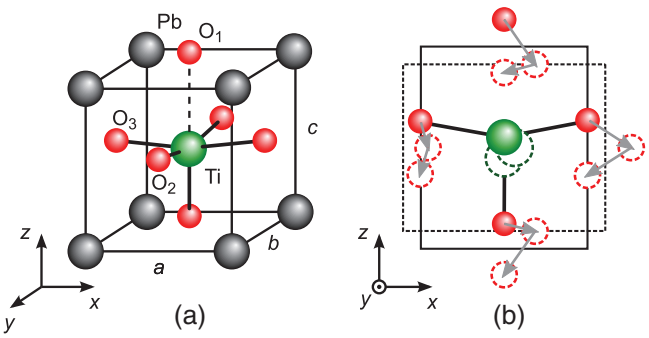

Figure 1. Tetragonal structure of $PbTiO_3$ (a) and its evolution (b) in (0 1 0) Ti-centered plane during the ferroelectric switching by polarization rotation.

parametrization of the energy surface (section 3) that makes our considerations more general. Next, we investigate an anisotropy of ferroelectric switching as a function of model parameters, which leads to determining optimal conditions for electrical excitations resulted in a reduced coercivity (section 4).

2 Mapping the energy surface

Below the Curie temperature, $PbTiO_3$ has a tetragonal structure shown in figure 1(a). The possible structural transformation corresponding to the polarization rotation in $PbTiO_3$ can involve an orthorhombic phase, which has the second lowest energy after the tetragonal one [10]. In this case, the polarization evolves in $\{0\,1\,0\}$ plane following the structural transformations path illustrated in figure 1(b). The change in atomic positions is accompanied by mechanically unconstrained changes of lattice parameters. Since the exact transition path is *a priori* unknown [12], the entire configurational space needs to be explored. With this purpose we introduce a two-dimensional configurational coordinate $\boldsymbol{\xi} = (\xi_x, \xi_z)$, which represents an arbitrary transition structure. The equilibrium tetragonal structures with the spontaneous polarization pointing 'up', 'down', 'left' and 'right' are represented by $\boldsymbol{\xi} = (0, +1)$, $(0, -1)$, $(-1, 0)$ and $(+1, 0)$, respectively; the centrosymmetric cubic structure corresponds to $\boldsymbol{\xi} = (0, 0)$. Atomic positions and lattice parameters (a and c) are then transformed according to

$$\boldsymbol{u}_{\mathrm{Ti}}(\xi_x, \xi_z) = \boldsymbol{u}_{\mathrm{Ti}}^{(\mathrm{C})} + \xi_z \left[\boldsymbol{u}_{\mathrm{Ti}}^{(\mathrm{T}_1)} - \boldsymbol{u}_{\mathrm{Ti}}^{(\mathrm{C})}\right] + \xi_x \left[\boldsymbol{u}_{\mathrm{Ti}}^{(\mathrm{T}_2)} - \boldsymbol{u}_{\mathrm{Ti}}^{(\mathrm{C})}\right]. \tag{1}$$

Here (T_1), (T_2) and (C) refer to the equilibrium structural parameters corresponding to tetragonal ('up' and 'right' polarization) and cubic structures, respectively.

The structural parameters of $PbTiO_3$ required for the calculation are gathered in table 1. The data presented were obtained with two approximations for the exchange correlation functional: the local density approximation (LDA) and Wu and Cohen [13] generalized gradient approximation (GGA-WC). As previously noticed by Balc *et al* [14], GGA-WC accurately reproduces the experimental low-temperature equilibrium volume of 63 Å^3 for tetragonal structure [15]. Both exchange-correlation functionals equally deviate from the experimental tetragonality ratio of $c/a = 1.07$ (LDA underestimates the value and GGA-WC overestimates it). However, LDA comes much closer to the spontaneous polarization of $P_\mathrm{s} \approx 0.75\,\mathrm{C\,m^{-2}}$ observed in $PbTiO_3$ at room temperature [16, 17]. Since polarization will later become one of the main model parameters, we proceed further with the LDA structure and comment on implications resulting from this particular choice where applicable.

Next we generate a set of structures that maps the configurational space within the range of $\xi_{x,y} \in [-1.2, +1.2]$ with the step size of $\Delta\xi = 0.1$ and compute their Kohn–Sham total energies as described in the appendix. The corresponding energy surface is shown in figure 2. The lowest energy corresponds to the tetragonal structures associated with four equivalent minima (only three are visible in figure 2). The cubic structure has the highest energy (excess of about 70 meV per unit cell). The obvious candidate for a transition state between tetragonal structures with the opposite polarization is an orthorhombic structure positioned at the saddle point connecting two adjacent tetragonal valleys. The energy for the orthorhombic structure is only 20 meV above the tetragonal one.

Our energy surface is consistent with the *ab initio* work of Hong and Vanderbilt [10] where the excess energies of 45 meV and 11 meV per unit cell were reported for the cubic and orthorhombic structures, respectively. The discrepancy can be attributed to the fact that both cubic and orthorhombic structures were fully optimized in [10], whereas we constrain the volume for all phases to its optimum value for the tetragonal phase. Although the volume variation is relatively small (less than 5%), its effect on the barrier height can be substantial.

Before we proceed with the discussion of external electric field effects, it will be useful to parametrize the energy surface in terms of the LD phenomenology.

3 LD parametrization

The free energy density of a ferroelectric crystal as a function of polarization $\boldsymbol{P}$ can be expressed as [18]

$$U_{\mathrm{LD}}(\boldsymbol{P}) = -\alpha P^2 + \beta P^4 + \gamma (P_x^2 P_y^2 + P_y^2 P_z^2 + P_x^2 P_z^2)\,, \tag{2}$$

where the energy for the parental cubic structure is taken as a reference. Here we limit the energy expansion to the fourth power in P, which is sufficient for description of the second-order phase transition [19].

The model parameters in equation (2) are not fully phenomenological, but can rather be related to material characteristics by

$$\alpha = \frac{2U_\mathrm{b}}{P_\mathrm{s}^2}, \qquad \beta = \frac{U_\mathrm{b}}{P_\mathrm{s}^4}, \qquad \gamma = \frac{4U_\mathrm{b}}{P_\mathrm{s}^4}\left(\frac{U_\mathrm{b}}{U_\mathrm{b}^*} - 1\right). \tag{3}$$

The coefficients α and β are expressed in terms of the T $\rightarrow$ C energy barrier height U_b and to the spontaneous polarization for the tetragonal phase P_s as previously established by Beckman *et al* [7]. The coefficient γ plays a crucial role in our study, since it is responsible for the directional anisotropy of the energy surface, which is parametrized with only one additional factor—U_b^* being the O $\rightarrow$ C energy barrier height.

Table 1. Structural parameters (fractional coordinates $\boldsymbol{u}$ and lattice constants a, b and c), spontaneous polarization (P_s) and the total energy difference (ΔE_{tot}) per unit cell relative to the cubic structure for $PbTiO_3$ in three distinct phases obtained from self-consistent *ab initio* calculations using LDA and GGA exchange-correlation functionals (see appendix for details).

Structural parameters	Tetragonal (T)	Orthorhombic[a] (O)	Cubic[b] (C)
LDA			
a, b, c (Å)	(3.858, 3.858, 4.039)	(3.955, 3.844, 3.955)	(3.918, 3.918, 3.918)
$\boldsymbol{u}_{Ti}$	(0.5, 0.5, 0.5328)	(0.5197, 0.5, 0.5197)	(0.5, 0.5, 0.5)
$\boldsymbol{u}_{O_1}$	(0.5, 0.5, 0.0902)	(0.5197, 0.5, 0.0541)	(0.5, 0.5, 0)
$\boldsymbol{u}_{O_2}$	(0.5, 0, 0.6023)	(0.5197, 0, 0.5197)	(0.5, 0, 0.5)
$\boldsymbol{u}_{O_3}$	(0, 0.5, 0.6023)	(0.0541, 0.5, 0.5197)	(0, 0.5, 0.5)
P_s (C m^{-2})	0.80	0.68	0
ΔE_{tot} (meV)	−72	−54	0
GGA-WC			
a, b, c (Å)	(3.872, 3.872, 4.220)	(4.059, 3.841, 4.059)	(3.985, 3.985, 3.985)
$\boldsymbol{u}_{Ti}$	(0.5, 0.5, 0.5387)	(0.5232, 0.5, 0.5232)	(0.5, 0.5, 0.5)
$\boldsymbol{u}_{O_1}$	(0.5, 0.5, 0.1189)	(0.5736, 0.5, 0.0713)	(0.5, 0.5, 0)
$\boldsymbol{u}_{O_2}$	(0.5, 0, 0.6227)	(0.5736, 0, 0.5736)	(0.5, 0, 0.5)
$\boldsymbol{u}_{O_3}$	(0, 0.5, 0.6227)	(0.0713, 0.5, 0.5736)	(0, 0.5, 0.5)
P_s (C m^{-2})	0.95	0.81	0
ΔE_{tot} (meV)	−153	−102	0

[a] Lattice constants and atomic positions are obtained by interpolation between cubic and tetragonal structures using equation (1) with $\boldsymbol{\xi} = (0.6, 0.6)$, which corresponds to the lowest total energy. The volume conservation is enforced when calculating the lattice parameter b.

[b] The same volume as for tetragonal structure is assumed.

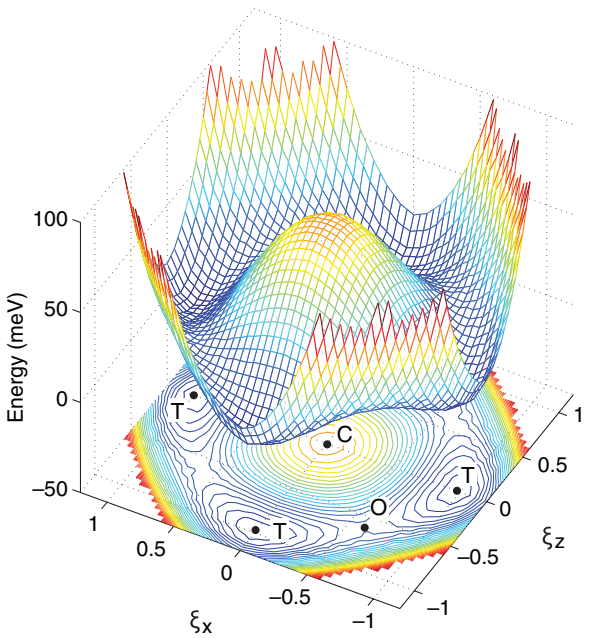

Figure 2. Energy surface calculated from first principles for the polarization inversion in (0 1 0) plane of $PbTiO_3$. The labels C, T and O refer to cubic, tetragonal and orthorhombic structures, respectively.

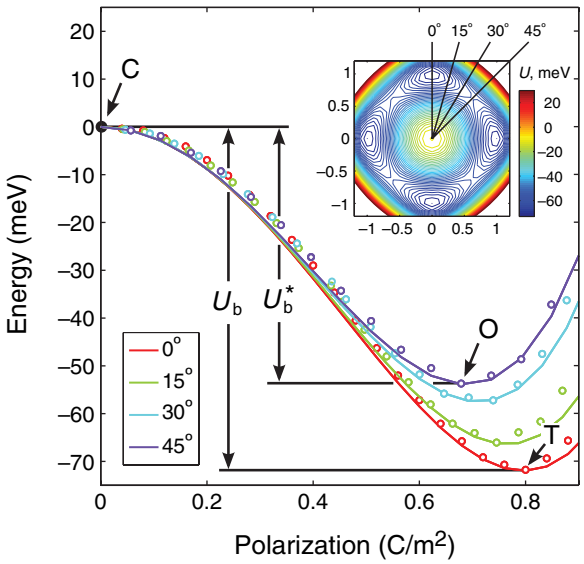

Figure 3. Directional anisotropy of the energy surface as a function of polarization $\sqrt{P_x^2 + P_z^2}$ sliced at different angles as shown in the inset. Solid lines represent fitting to equation (2) with parameters described in the text. The barrier heights U_b and U_b^* associated with transition between cubic (C), tetragonal (T) and orthorhombic (O) structures are shown.

In order to enable further analysis of external electric field effects, the energy surface presented on figure 2 needs to be recast in a polarization representation. With this purpose we calculate the polarization using the Berry phase approach [20] for individual structures that span our region of interest in the $\boldsymbol{\xi}$-space (details are given in the appendix). Results for fitting of the *ab initio* energy surface to the free energy functional given by equation (2) are presented in figure 3. The best fit corresponds to the following set of parameters: $\alpha = 600\,\text{MJ m C}^{-2}$, $\beta = 480\,\text{MJ m}^5\,\text{C}^{-4}$ and $\gamma = 640\,\text{MJ m}^5\,\text{C}^{-4}$.

We would like to note that the values of LD parameters are sensitive to the choice of exchange-correlation functional and/or the approach for optimization of intermediate structures along the polarization switching path. Further improvement in the accuracy of mapping the energy surface can be achieved by lifting the constant volume restriction implied above. As a result, one can anticipate a flatter energy surface (lower α)

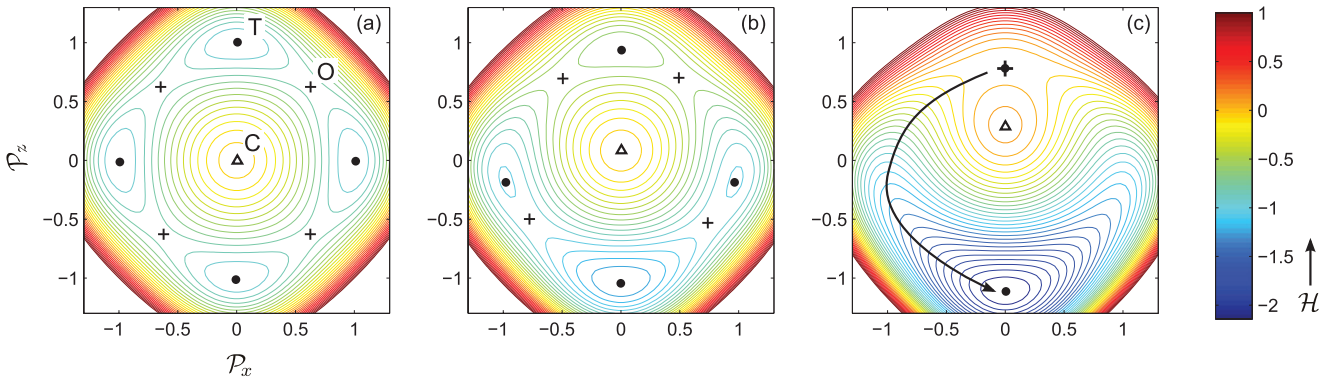

Figure 4. Energy surface $\mathcal{H}$ modified by a uniaxial external electric field $\mathcal{E}_z$ of varying magnitude: (*a*) $\mathcal{E}_z = 0$, (*b*) $\mathcal{E}_z = -0.5$ and (*c*) $\mathcal{E}_z = -1.1$. Notice changes in the position of stationary points (minima (•), maxima (△) and saddle points (+)) caused by the external field. The arrow on (*c*) illustrates the polarization rotation. The labels C, T and O refer to cubic, tetragonal and orthorhombic structures, respectively. The energy surface is shown for the anisotropy factor $k = 0.25$.

combined with a less pronounced directional anisotropy (lower γ). This is exactly what we see from the energy profile data reported in [10] that yield an alternative set of parameters for $PbTiO_3$, namely $\alpha = 420\,\mathrm{MJ\,m\,C^{-2}}$, $\beta = 350\,\mathrm{MJ\,m^5\,C^{-4}}$ and $\gamma = 280\,\mathrm{MJ\,m^5\,C^{-4}}$.

4 Polarization switching

The effect of an external electric field $\boldsymbol{E}$ on the energy profile can be taken into account by adding an electrostatic potential energy. Then the resultant energy functional (electric enthalpy) takes the form [10, 21]

$$H(\boldsymbol{E}, \boldsymbol{P}) \approx U(\boldsymbol{P}) - \boldsymbol{E} \cdot \boldsymbol{P}. \tag{4}$$

Here $U(\boldsymbol{P})$ represents the free energy for a system in a particular polarization state that can be determined either from first principles or using the LD parametrization. Here we neglect an effect of the external electric field on the free energy. This approach can be justified in the case of ferroelectrics, where the polarization and its response to the electric field is strongly dominated by ionic contribution in the frequency range of $f \lesssim 100\,\mathrm{MHz}$ [22].

In order not to restrict our results to a particular choice of material parameters, it is convenient to define dimensionless quantities

$$\mathcal{P} = \frac{P}{P_\mathrm{s}}, \qquad \mathcal{E} = \frac{E P_\mathrm{s}}{U_\mathrm{b}}, \qquad \mathcal{H} = \frac{H}{U_\mathrm{b}} \tag{5}$$

associated with the reduced polarization $\mathcal{P}$, electric field $\mathcal{E}$ and energy density $\mathcal{H}$.

4.1 Uniaxial electric field

Let us assume that the external electric field points along $[0\,0\,\bar{1}]$ crystallographic direction antiparallel to the spontaneous polarization. The field breaks the original four fold symmetry of the energy surface (figure 4(*a*)). As the field increases, the stationary points (T, O and C) displace from their zero-field positions as shown in figure 4(*b*). Such an evolution represents a modification of the equilibrium structural parameters caused by the external electric field, which is the essence of piezoelectric effect. The switching takes place when the energy of the tetragonal structure merges with that for the orthorhombic structure (figure 4(*c*)).

As we proceed with derivation of the coercive electric field for ferroelectric switching, the Landau–Devonshire parametrization equation (2) for the free energy will be used in order to keep the results general. The position of stationary points correspond to zero gradient of the enthalpy surface

$$\frac{\partial U_\mathrm{LD}(\boldsymbol{P})}{\partial P_z} = E_z, \tag{6a}$$

$$\frac{\partial U_\mathrm{LD}(\boldsymbol{P})}{\partial P_x} = E_x. \tag{6b}$$

This set of equations has generally nine sets of solutions $\{P_x(E_x, E_z), P_z(E_x, E_z)\}$ as shown in figure 4(*b*). The condition for switching by polarization rotation is

$$P_x^{(\mathrm{T})} = P_x^{(\mathrm{O})} \qquad \text{and} \qquad P_z^{(\mathrm{T})} = P_z^{(\mathrm{O})}. \tag{7}$$

With the assumption of $E_x = 0$, equations (6) and (7) yield the following result for the coercive field in terms of the model parameters:

$$E_{\mathrm{c,\,rot}} = 2\gamma \left(\frac{\alpha}{2\beta + \gamma}\right)^{3/2} = 8k(1+2k)^{-3/2}\frac{U_\mathrm{b}}{P_\mathrm{s}}, \tag{8}$$

where $k = (U_\mathrm{b}/U_\mathrm{b}^* - 1)$ is a coefficient that appears in equation (3) and characterizes the degree of anisotropy of the free energy surface. This result indicates that the coercive field is largely determined by the energy surface anisotropy and vanishes for an isotropic energy surface ($\gamma = 0$ or $k = 0$) as shown in figure 5 (solid line).

The coercivity approaches its maximum at $\gamma = 4\beta$ ($k = 1$ in figure 5). In this limit, we recover the coercive field for polarization flip through the cubic structure obtained earlier by Kim *et al* [6]

$$E_{\mathrm{c,\,fl}} = (2\alpha/3)^{3/2}\beta^{-1/2} = \frac{8}{3^{3/2}}\frac{U_\mathrm{b}}{P_\mathrm{s}}. \tag{9}$$

The following condition needs to be fulfilled for polarization rotation to remain an energetically favorable mechanism for ferroelectric switching:

$$\frac{U_\mathrm{b}}{U_\mathrm{b}^*} < 2. \tag{10}$$

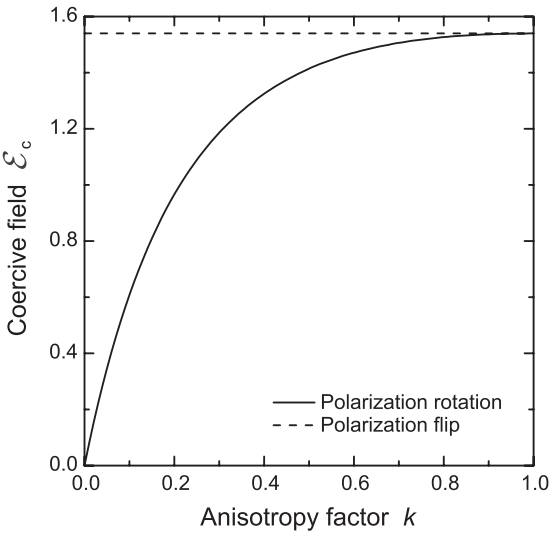

Figure 5. Coercive field for ferroelectric switching as a function of the energy surface anisotropy. Uniaxial electric field is assumed ($\mathcal{E}_x = \mathcal{E}_y = 0$).

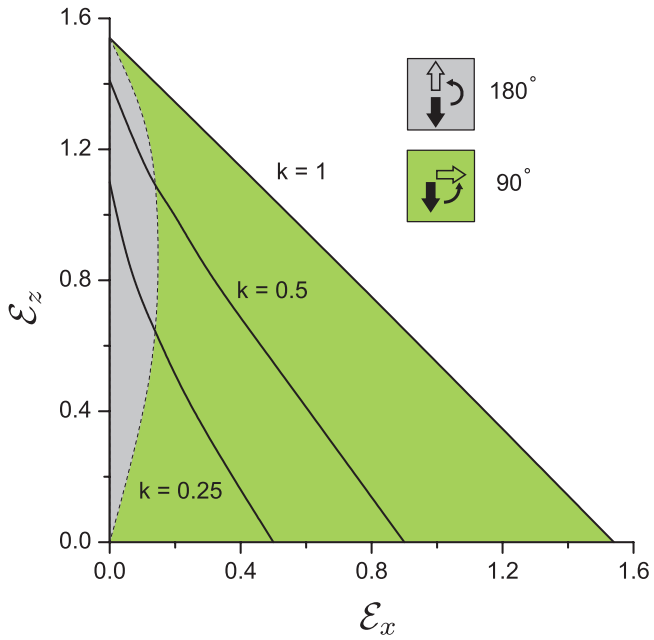

Figure 6. Coercive field for ferroelectric switching via polarization rotation in response to a biaxial external electric field as a function of the anisotropy factor k. The shaded regions distinguish between areas with the full polarization inversion (180° rotation) and partial switching (90° rotation).

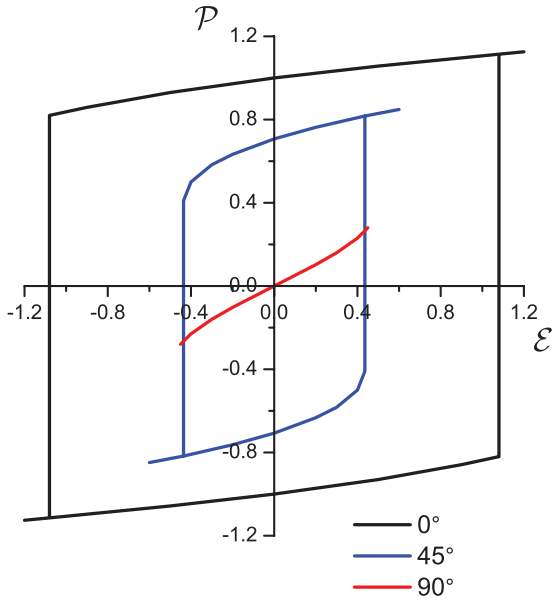

Figure 7. Directional anisotropy of the ferroelectric hysteresis. The angle is measured between the electric field direction and the axis of spontaneous polarization.

This result implies that the switching via orthorhombic state is favorable when the corresponding barrier is lower at least by a factor of *two* in comparison to the barrier for polarization flip via the cubic structure.

The energy surface of $PbTiO_3$ calculated here with LDA yields the ratio of $U_b/U_b^* = 1.33$ (1.20 for the surface in [10]) that clearly favors the polarization rotation. In spite of the fact that the energy barrier for the polarization switching via orthorhombic structure is as low as 1/5–1/3 of a corresponding value for the cubic structure, the coercive field is reduced by 20–40% only in comparison to the switching by polarization flip (compare data in figure 5 at $k = 0.2$–0.33 and $k = 1$). Such a high resistance to ferroelectric switching can be attributed to the absence of a tangential component of the external electric field E_x to the curved switching path (figure 4(*c*)).

4.2 Coercive field anisotropy

The coercive field for an arbitrary direction $\boldsymbol{E}$ can be obtained by solving the set of equations (6*a*) and (6*b*) numerically. The results are presented in figure 6 for three distinct values of the anisotropy parameter k.

The coercive field has the highest magnitude when aligned with the direction of spontaneous polarization (z), which is analogous to a 'hard' axis in ferromagnets [23]. The field is greatly reduced when its direction deviates from this axis (figure 6). The reduction is more pronounced in materials with a lower anisotropy of the energy surface. Here two types of switching should be distinguished: 180° and 90°. The former corresponds to a complete polarization inversion, whereas the latter represents switching between two states with the mutually orthogonal polarization (an intermediate state shown in figure 1). The relevant switching mechanism is identified with a background color in figure 6. Apparently, the 180° polarization inversion is observed only in a narrow range of fields near to the hard axis.

Since the coercive field is highly anisotropic, it is anticipated that the ferroelectric hysteresis will also be sensitive to the direction of applied electric field. Figure 7 presents two hysteresis curves calculated for an energy surface with $k = 0.25$ with the external field applied along the hard (0°) and easy (45°) axis. The ferroelectric switching along the easy axis exhibits lower coercivity, but also smaller change in the polarization and, consequently, a lower mechanical response. In order to take the advantage of reduced coercivity and maximize the mechanical response at the same time, both direction and magnitude of the field need to be manipulated during the switching cycle.

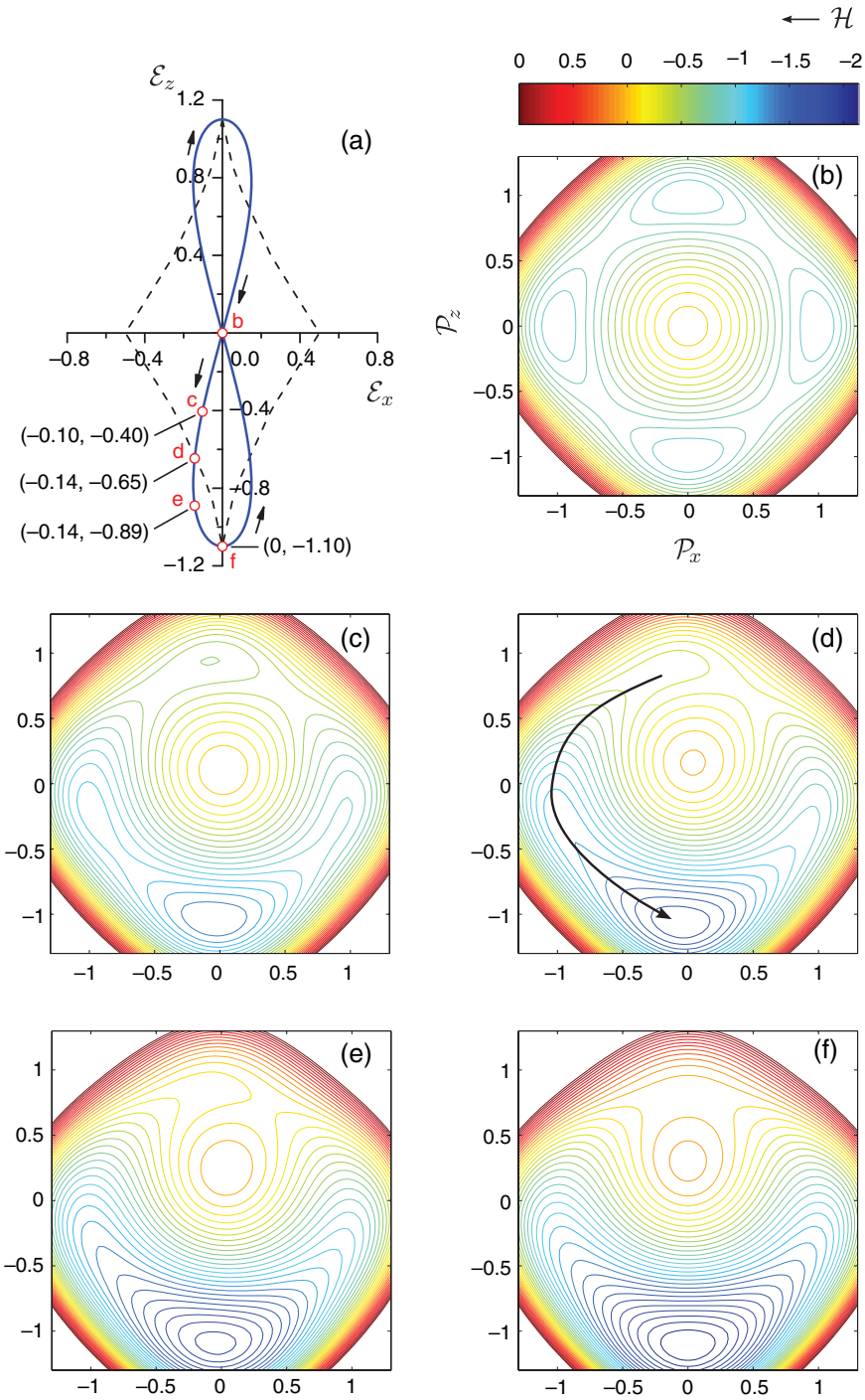

Figure 8. 180° ferroelectric switching driven by a lemniscate-like rotating electric field (*a*). Individual panels (*b*)–(*f*) represent the energy surface $\mathcal{H}$ for particular excitation states with individual components of the electric field $\mathcal{E}$ labeled on (*a*). Since the direction of electric field deviates from the hard axis, the switching occurs at a lower field (*d*). The anisotropy factor $k = 0.25$ is used for generating the energy surface.

5 Discussion

Although, the results presented above are specific to the polarization rotation in $\{0\,1\,0\}$ plane, the arguments can be readily extended to other compounds with the energy surface similar to that shown in figure 2. For example, the polarization rotation in PZT takes place in $\{1\,1\,0\}$ plane and involves transition between tetragonal, rhombohedral and orthorhombic phases. The energy of tetragonal and rhombohedral phases approach each other near to MPB resulting in a flatter energy surface [1, 4], i.e. lower k-factor. The latter should lead to a lower coercivity near to MPB (figure 5) and a pronounced anisotropy of the coercive field following the analogy with figure 6.

Experimental studies of the polarization rotation in pre-poled $Pb(Zr,Ti)O_3$ samples subjected to an electric field at different angles with respect to the original poling direction were reported in the literature [24–26]. According to these

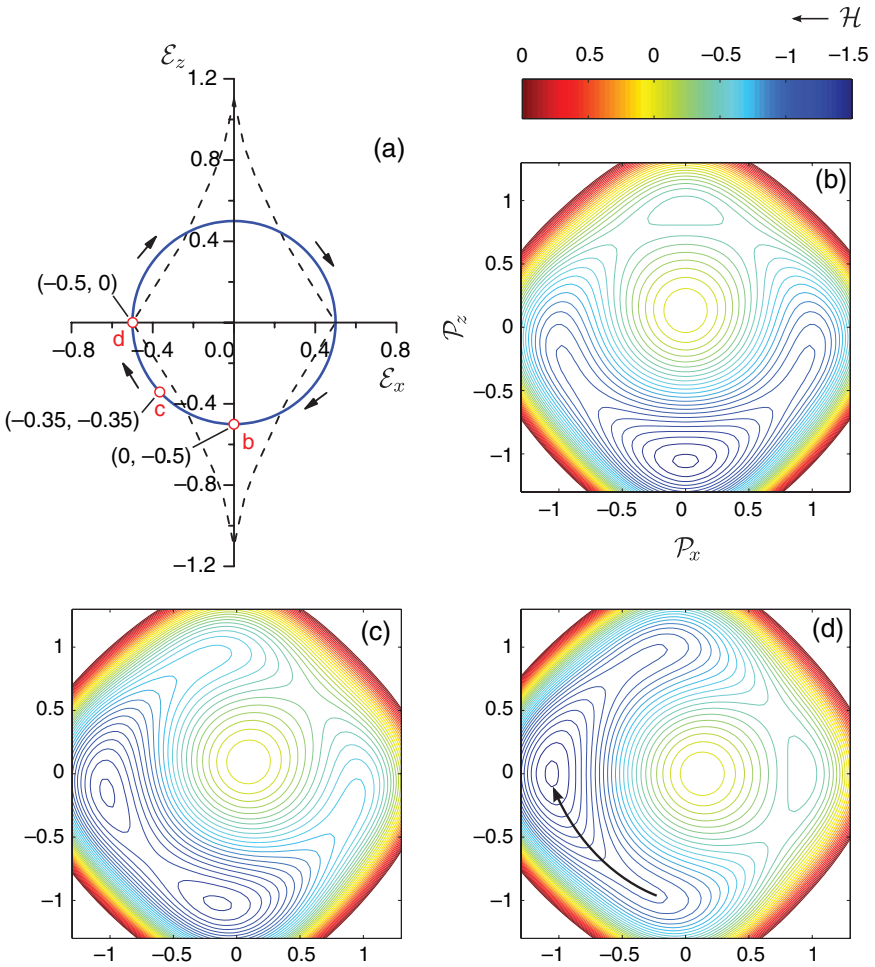

Figure 9. 90° ferroelectric switching driven by a circularly rotating electric field (*a*). Individual panels (*b*)–(*d*) represent the energy surface $\mathcal{H}$ for particular excitation states with individual components of the electric field $\mathcal{E}$ labeled on (*a*). Since the direction of electric field deviates from the hard axis, the switching occurs at a lower field (*d*). The anisotropy factor $k = 0.25$ is used for generating the energy surface.

studies, the highest coercivity and highest polarization change are observed when attempting to switch the polarization by applying the field antiparallel to the poling axis. The coercivity and the saturated polarization are reduced as the direction of applied field deviates from this axis. These observations are consistent with our model.

Commonly used ferroelectric actuators are driven by applying the electric field along a poling axis in order to maximize their mechanical response [27]. A possible strategy for reduction of the coercivity while maintaining the high mechanical response is to employ a two-dimensional excitation with an active modulation of $E_x(t)$ and $E_z(t)$ components of the applied field. When aiming at 180° switching, the electric field vector should be confined within the gray area in figure 6. This can be achieved with a time-varying field $\boldsymbol{E}(t)$, which takes a shape of the lemniscate-like parametric curve shown in figure 8(*a*). The advantage of such a two-dimensional excitation is that the switching takes place at a lower field (*d*-point), while the maximum longitudinal mechanical response is expected at f-point where the field reaches its maximum, and the transverse component is eliminated (see figure 8(*f*)).

Sequential 90° polarization switching events were previously identified as possible nucleation centers for new domains [28]. The lowest coercivity can be anticipated when the polarization inversion is driven by a circular excitation (figure 9). A high tangential component of the rotating electric field causes the polarization inversion via a series of successive 90° switching steps. Under such circumstances, both longitudinal and lateral modes of excitation alternate resulting in the alternating mechanical response in two dimensions. However, it should be noted that 90° polarization reorientation was previously identified as a source for mechanical energy losses and damping [29], which can produce an adverse impact on the performance of high power ultrasonic actuators operated at resonance.

Finally we would like to note on applicability of our results in the case when a particular experimental situation does not fully correspond to the model assumptions studied here, namely a single-domain switching in the absence of mechanical constraints. The majority of technologically relevant ferroelectrics are random, sintered polycrystals with a variety of crystallographic orientations present in a bulk sample [24]. Individual grains behave as a single domain when their size does not exceed 150 nm [30]; larger grains exhibit a multidomain structure. Atomic scale simulations [31] show that an evolution of the polarization vector across the

domain boundary resembles the polarization rotation discussed above. Among various domain structures (see, e.g., [32] and references therein), 90° zig-zag domain configuration is often reported in experimental studies [33–36]. This observation can be attributed to the low coercivity of 90° polarization rotation (figure 6) combined with a markedly lower formation energy of 90° domain boundaries evaluated by Meyer and Vanderbilt [31].

6 Conclusions

$PbTiO_3$ was used as a model system to study a single-domain polarization rotation in tetragonal perovskite structures. The energy surface for the polarization rotation in {0 1 0} plane was mapped using *ab initio* calculations and then parametrized using a Landau–Devonshire phenomenology. We show that the coercive field exhibits a strong directional anisotropy, which is determined by an anisotropy of the energy surface. A lower energy anisotropy leads to a lower coercivity. Switching of polarization by 180° requires the highest external electric field, which should be aligned with the tetragonal *c*-axis within approximately 10°–15°. The *c*-axis plays a role of the hard axis similar to a magnetic anisotropy. For random crystallographic orientations, the ferroelectric switching will likely take place via 90° polarization rotation at a fraction of the coercive field required for 180° polarization inversion. Eventually, a two component rotating electric field is proposed as an excitation method, which is expected to facilitate the switching process.

Acknowledgments

Authors would like to acknowledge funding provided by the Natural Sciences and Engineering Research Council of Canada under the Discovery Grant Program 386018-2010 and the Ontario Ministry of Economic Development and Innovation under the Ontario Research Fund program (ORF-2). JC wants to thank the Northern Ontario Heritage Fund Corporation for the support via a Youth Internship and Co-Op program.

Appendix. Electronic structure calculations

The first-principles calculations were carried out using the density-functional theory and a linear augmented plane wave basis set implemented in `WIEN2K` package [37]. The local spin density approximation [38] as well as the Wu and Cohen [13] generalized gradient approximation have been used in this study for the exchange correlation functional. The Brillouin zone was sampled using $6 \times 6 \times 6$ *k*-mesh. The radii R_{MT} of muffin tin spheres centered at individual atoms were chosen to be equal 2.26 Bohr, 1.68 Bohr and 1.49 Bohr for Pb, Ti and O, respectively. The product of the minimum R_{MT} radius and the maximum cut-off wave vector in the reciprocal space was kept at the constant value of $R_{MT}K_{max} = 7$ throughout all calculations. The energy to separate core and valence electron was set such that electrons in the following orbitals were treated as valence electrons: Pb—5p 5d 6s 6p, Ti—3s 3p 3d 4s and O—2s 2p.

The fully optimized self-consistent structural parameters for tetragonal $PbTiO_3$ were used in the calculations (table 1). The internal degrees of freedom for the tetragonal structure of $PbTiO_3$ were fully relaxed by minimizing the Hellmann–Feynman forces acting on atoms below 0.2 mRy $Bohr^{-1}$.

Polarization properties were calculated based on the modern theory of polarization [20] in the framework of Berry phase approach [39]. This capability is implemented in a `BerryPI` package [40] for `WIEN2k` used in conjunction with a `WIEN2WANNIER` package [41].

References

[1] Damjanovic D 2005 *J. Am. Ceram. Soc.* **88** 2663
[2] Budimir M, Damjanovic D and Setter N 2006 *Phys. Rev.* B **73** 174106
[3] Bell A J 2007 Factors influencing the piezoelectric behaviour of PZT and other 'morphotropic phase boundary' ferroelectrics *Frontiers of Ferroelectricity* (New York: Springer) pp 13–25
[4] Damjanovic D 2010 *Appl. Phys. Lett.* **97** 062906
[5] Ducharme S, Fridkin V M, Bune A V, Palto S P, Blinov L M, Petukhova N N and Yudin S G 2000 *Phys. Rev. Lett.* **84** 175
[6] Kim S, Gopalan V and Gruverman A 2002 *Appl. Phys. Lett.* **80** 2740
[7] Beckman S P, Wang X, Rabe K M and Vanderbilt D 2009 *Phys. Rev.* B **79** 144124
[8] Fu H and Cohen R E 2000 *Nature* **403** 281
[9] Noheda B, Cox D E, Shirane G, Park S-E, Cross L E and Zhong Z 2001 *Phys. Rev. Lett.* **86** 3891
[10] Hong J and Vanderbilt D 2011 *Phys. Rev.* B **84** 115107
[11] Taherinejad M, Vanderbilt D, Marton P, Stepkova V and Hlinka J 2012 *Phys. Rev.* B **86** 155138
[12] Marton P, Rychetsky I and Hlinka J 2010 *Phys. Rev.* B **81** 144125
[13] Wu Z and Cohen R E 2006 *Phys. Rev.* B **73** 235116
[14] Bilc D I, Orlando R, Shaltaf R, Rignanese G-M, Íñiguez J and Ghosez P 2008 *Phys. Rev.* B **77** 165107
[15] Glazer A and Mabud S 1978 *Acta Crystallogr.* B **34** 1065
[16] Gavrilyachenko V G, Spinko R I, Martynenko M A and Fesenko E G 1970 *Sov. Phys.—Solid State* **12** 1203
[17] Akdogan E K, Mayo W, Safari A, Rawn C and Payzant E 1999 *Ferroelectrics* **223** 11
[18] Devonshire A 1949 *Phil. Mag.* **40** 1040
[19] Cao W 2008 *Ferroelectrics* **375** 28
[20] King-Smith R D and Vanderbilt D 1993 *Phys. Rev.* B **47** 1651
[21] Nunes R W and Vanderbilt D 1994 *Phys. Rev. Lett.* **73** 712
[22] Jiwei Z, Xi Y, Mingzhong W and Liangying Z 2001 *J. Phys. D: Appl. Phys.* **34** 1413
[23] Stoner E C and Wohlfarth E P 1948 *Phil. Trans R. Soc. Lond.* A **240** 599
[24] Huber J E and Fleck N A 2001 *J. Mech. Phys. Solids* **49** 785
[25] Huber J E, Shieh J and Fleck N A 2002 *Proc. SPIE* **4699** 133
[26] Zhou D, Kamlah M and Laskewitz B 2006 *Proc. SPIE* **6170** 617009
[27] Haertling G H 1999 *J. Am. Ceram. Soc.* **82** 797
[28] Xia Y and Wang J 2012 *Smart Mater. Struct.* **21** 094019
[29] Uchino K, Zheng J H, Chen Y H, Du X H, Ryu J, Gao Y, Ural S, Priya S and Hirose S 2006 *J. Mater. Sci.* **41** 217
[30] Ren S B, Lu C J, Liu J S, Shen H M and Wang Y N 1996 *Phys. Rev.* B **54** R14337
[31] Meyer B and Vanderbilt D 2002 *Phys. Rev.* B **65** 104111
[32] Chou C-C and Chen C-S 2000 *Ceram. Int.* **26** 693

[33] Merz W J 1954 *Phys. Rev.* **95** 690
[34] Arlt G *et al* 1985 *J. Appl. Phys.* **58** 1619
[35] Chou C-C, Hou C-S and Yeh T-H 2005 *J. Eur. Ceram. Soc.* **25** 2505
[36] Catalan G, Schilling A, Scott J F and Gregg J M 2007 *J. Phys.: Condens. Matter* **19** 132201
[37] Blaha P, Schwarz K, Madsen G K H, Kvasnicka D and Luitz J 2001 *Wien2k: An Augmented Plane Wave + Local Orbitals Program for Calculating Crystal Properties* (Karlheinz Schwarz, Techn. Universität Wien, Austria)
[38] Perdew J P and Wang Y 1992 *Phys. Rev.* B **45** 13244
[39] Berry M V 1984 *Proc. R. Soc. Lond.* A **392** 45
[40] Ahmed S, Kivinen J, Zaporzan B, Curiel L, Pichardo S and Rubel O 2013 *Comput. Phys. Commun.* **184** 647
[41] Kunes J, Arita R, Wissgott P, Toschi A, Ikeda H and Held K 2010 *Comput. Phys. Commun.* **181** 1888